Journal of ELECTRICAL ENGINEERING, VOL. 56, NO. 3-4, 2005, 57–63

NONLINEAR FEEDBACK CONTROL AND TORQUE OPTIMIZATION OF A DOUBLY FED INDUCTION MOTOR

Saïd Drid * — Mohamed Tadjine ** — Mohamed-Said Naït-Saïd *

In this paper, the authors propose a new vector control intended for doubly fed induction motor (DFIM) mode. The use of the state-all-flux induction machine model with a fluxes orientation constraint gives place to a simpler control model. Since the double flux orientation creates an orthogonally between the stator and rotor fluxes, it results a linear and decoupled machine control giving an optimal developed torque. The nonlinear feedback control purpose is employed and where the global asymptotic control stability is proven using the Lyapunov function. The present DFIM-control is achieved by means of armature fluxes, so the machine saturation should be mostly solicited. Consequently, a new torque-optimization- factor (TOF) will be proposed in this work.

Keywords: double fed induction machine, wound rotor, vector control, flux orientation, Lyapunov function, torque-optimization-factor (TOF), energy saving

1 NOMENCLATURE

s, r	Rotor and stator indices
d, q	Direct and quadrate indices for orthogonal components
$\bar{x}$	Variable complex such as: $\bar{x} = \Re e\,[\bar{x}] + j\ \Im m\,[\bar{x}]$ with $j^2 = -1$
$\bar{x}$	It can be a voltage as $\bar{u}$, a current as $\bar{i}$ or a flux as $\bar{\phi}$
$\bar{x}^*$	Complex conjugate
R_s, R_r	Stator and rotor resistances
L_s, L_r	Stator and rotor inductances
T_s, T_r	Stator and rotor time-constants ($T_{s,r} = L_{s,r}/R_{s,r}$)
σ	Leakage flux total coefficient ($\sigma = 1 - M^2/L_r L_s$)
M	Mutual inductance,
θ	Absolute rotor position
P	Number of pairs poles
δ	Torque angle
ρ_s, ρ_r	Stator and rotor flux absolute positions
ω	Mechanical rotor frequency (rd/s)
Ω	Rotor speed (rd/s)
ω_s	Stator current frequency (rd/s)
ω_r	Induced rotor current frequency (rd/s)
ω_c	Injected rotor current frequency (rd/s)
J	Inertia
C_r	Load torque
C_e	Electromagnetic torque
$\sim$	Symbol indicating measured value
$\hat{}$	Symbol indicating the estimated value
*	Symbol indicating the command value
DFIM	Doubly Fed Induction Machine
TOF	Torque Optimization Factor

2 INTRODUCTION

Known since 1899 [1], the doubly fed induction machine (DFIM) is a wound rotor asynchronous machine supplied by the stator and the rotor from two external source voltages. This solution is very attractive for the variable speed applications such as the electric vehicle and the electrical energy production [1–5]. Consequently, it covers all powers ranges. Obviously, the requested variable speed domain and the desired performances depend of the application kinds [1–7]. The use of DFIM offers the opportunity to modulate power flow into and out the rotor winding in order to have, at the same time, a variable speed in the characterized super-synchronous or sub-synchronous modes in motor or in generator regimes. Two modes can be associated to slip power recovery: sub-synchronous motoring and super-synchronous generating operations. In general, while the rotor is fed through a cycloconverter, the power range can attain the MW order which presents the size power often reserved to the synchronous machine. [1-10].

The DFIM has some distinct advantages compared to the conventional squirrel-cage machine. The DFIM can be controlled from the stator or rotor by various possible combinations. The disadvantage of two used converters for stator and rotor supplying can be compensated by the best control performances of the powered systems [3]. Indeed, the input-commands are done by means of four precise degrees of control freedom relatively to the squirrel cage induction machine where its control appears quite simpler. The flux orientation strategy can transform the non linear and coupled DFIM-mathematical model to a linear model leading to one attractive solution as well as under generating or motoring operations [1–15].

The main idea behind all flux orientation control strategies is that the machine flux position or vector flux components are computed from the direct physic measurements. In DFIM, both stator and rotor currents are easily measured, at that moment the flux vectors

* Laboratory of Electromagnetic Induction and Propulsion Systems, Electrical engineering department; University of Batna, Rue M.E.H Boukhlof, Algeria, e-mail: s_drid@lycos.com, ms.naitsaid@Lycos.com

** Process Control Laboratory, Electrical engineering department, ENP Algiers, 10 Av. Hassen Badi, B182. Algiers, Algeria, e-mail: tadjine@yahoo.fr

ISSN 1335-3632

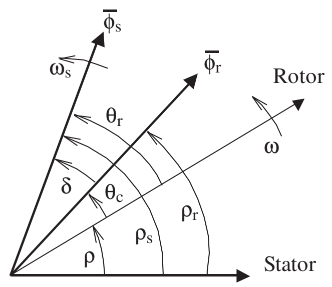

Fig. 1. DFIM flux relative armature position

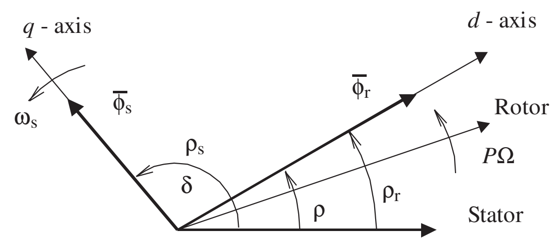

Fig. 2. DFIM vectorial diagram after orientation

can be calculated using non differential equations flux-current constituting a simpler flux estimator. It depends on inductive parameters (inductances) which are function on the machine saturation state. Its robustness against saturation effect could be guaranteed by the torque-optimization-factor (TOF) which will be exposed, in the next. In this work, to solve the problem of non linear DFIM control, the solution of non linear feedback control was adopted in order to create a double flux orientation applied for all-flux induction machine model. It results that the stator flux oriented in q-axis becomes the active power input command from which the developed torque will be controlled, while the rotor flux assumes the reactive power input command acting the magnetizing machine system.

Since the fluxes are used like control variables, the machine fluxes must be maintained at acceptable level especially during the transient regimes. Then the transient torque time evolution should be optimized during the rapid change of variables command (fluxes) which can reach very high magnitude. So a new torque-optimization-factor (TOF) will be proposed in this work. The main function of this controller is to optimize the transient torque in keeping the machine saturation at the acceptable level. Thereafter, the machine current magnitudes will be sufficiently reduced with their accompanied copper losses guaranteeing improved machine efficiency.

3 THE DFIM MODEL

Its dynamic model expressed in the synchronous reference frame is given by Voltage equations:

$$\begin{aligned} \bar{u}_s &= R_s \bar{i}_s + \frac{\mathrm{d}\bar{\phi}_s}{\mathrm{d}t} + j\omega_s \bar{\phi}_s \,, \\ \bar{u}_r &= R_r \bar{i}_r + \frac{\mathrm{d}\bar{\phi}_r}{\mathrm{d}t} + j\omega_r \bar{\phi}_r \,. \end{aligned} \tag{1}$$

Flux equations:

$$\begin{aligned} \bar{\phi}_s &= L_s \bar{i}_s + M \bar{i}_r \,, \\ \bar{\phi}_r &= L_r \bar{i}_r + M \bar{i}_s \,. \end{aligned} \tag{2}$$

From (1) and (2), the state-all-flux model is written like

$$\begin{aligned} \bar{u}_s &= \frac{1}{\sigma T_s}\bar{\phi}_s - \frac{M}{\sigma T_s L_r}\bar{\phi}_r + \frac{\mathrm{d}\bar{\phi}_s}{\mathrm{d}t} + j\omega_s\bar{\phi}_s \,, \\ \bar{u}_r &= -\frac{M}{\sigma T_r L_s}\bar{\phi}_s + \frac{1}{\sigma T_r}\bar{\phi}_r + \frac{\mathrm{d}\bar{\phi}_r}{\mathrm{d}t} + j\omega_r\bar{\phi}_r \,. \end{aligned} \tag{3}$$

The electromagnetic torque is done as

$$C_e = \frac{PM}{\sigma L_s L_r} \Im m \left[\bar{\phi}_s \bar{\phi}_r^*\right] \tag{4}$$

and its associated motion equation is:

$$C_{el} - C_r = J\frac{\mathrm{d}\Omega}{\mathrm{d}t} \,. \tag{5}$$

In DFIM operations, the stator and rotor mmf's (magneto motive forces) rotations are directly imposed by the two external voltage source frequencies. Hence, the rotor speed becomes depending toward the linear combination of theses frequencies, and it will be constant if they are too constants for any load torque, given of course in the machine stability domain. In DFIM modes, synchronization between both fmm's is mainly required in order to guarantee machine stability [5]. This is the similar situation of the synchronous machine stability problem where without the recourse to the strict control of the DFIM fmm's relative position, the machine instability risk or brake down mode become imminent. Figure 1 illustrates the DFIM flux relative positions; particularly we can distinguish the torque angle δ defined between them. This angle denotes, by analogy to the synchronous machine, the torque angle. Each flux is located by a relative armature position.

4 DFIM DOUBLE FLUX ORIENTATION STRATEGY

A. Double flux orientation

It consists in orienting, at the same time, stator flux and rotor flux as indicated in Fig. 2. Thus, it results the constraints given below by (6). Rotor flux is oriented on the d-axis, and the stator flux is oriented on the q-axis. Conventionally, the d-axis remains reserved to magnetizing axis and q-axis to torque axis. Consequently, δ will be identical to 90° and the two fluxes become orthogonal, so we can write

$$\begin{aligned}\phi_{sq} &= \phi_s\,,\\ \phi_{rd} &= \phi_r\,,\\ \phi_{sd} &= \phi_{rq} = 0\,.\end{aligned} \tag{6}$$

Using (6), the developed torque given by (4) can be rewritten as follows:

$$C_{el} = k_c\phi_s\phi_r \tag{7}$$

where, $k_c = \frac{PM}{\sigma L_s L_r}$, ϕ_s appears as the input command of the active power or simply of the developed torque, while ϕ_r appears as the input command of the reactive power or simply the main magnetizing machine system acting.

B. Nonlinear feedback control for Double flux orientation

Separating the real-part and the imaginary-part of (3), one will have

$$\begin{aligned}u_{sd} &= \gamma_1\phi_{sd} - \gamma_2\phi_{rd} + \frac{\mathrm{d}\phi_{sd}}{\mathrm{d}t} - \omega_s\phi_{sq} = -f_1 + \frac{\mathrm{d}\phi_{sd}}{\mathrm{d}t},\\ u_{sq} &= \gamma_1\phi_{sq} - \gamma_2\phi_{rq} + \frac{\mathrm{d}\phi_{sq}}{\mathrm{d}t} + \omega_s\phi_{sd} = -f_2 + \frac{\mathrm{d}\phi_{sq}}{\mathrm{d}t},\\ u_{rd} &= -\gamma_3\phi_{sd} + \gamma_4\phi_{rd} + \frac{\mathrm{d}\phi_{rd}}{\mathrm{d}t} - \omega_r\phi_{rq} = -f_3 + \frac{\mathrm{d}\phi_{rd}}{\mathrm{d}t},\\ u_{rq} &= -\gamma_3\phi_{sq} + \gamma_4\phi_{rq} + \frac{\mathrm{d}\phi_{rq}}{\mathrm{d}t} + \omega_r\phi_{rd} = -f_4 + \frac{\mathrm{d}\phi_{rq}}{\mathrm{d}t}\end{aligned} \tag{8}$$

where $\gamma_1 = \frac{1}{\sigma T_s}$; $\gamma_2 = \frac{M}{\sigma T_s L_r}$; $\gamma_3 = \frac{M}{\sigma T_r L_s}$; $\gamma_4 = \frac{1}{\sigma T_r}$ and,

$$\begin{aligned}-f_1 &= \gamma_1\phi_{sd} - \gamma_2\phi_{rd} - \omega_s\phi_{sq}\,,\\ -f_2 &= \gamma_1\phi_{sq} - \gamma_2\phi_{rq} + \omega_s\phi_{sd}\,,\\ -f_3 &= -\gamma_3\phi_{sd} + \gamma_4\phi_{rd} - \omega_r\phi_{rq}\,,\\ -f_4 &= -\gamma_3\phi_{sq} + \gamma_4\phi_{rq} + \omega_r\phi_{rd}\,.\end{aligned} \tag{9}$$

Hence, (8) is simply rewritten as

$$\begin{aligned}\frac{\mathrm{d}\phi_{sd}}{\mathrm{d}t} &= f_1 + u_{sd}\,, & \frac{\mathrm{d}\phi_{sq}}{\mathrm{d}t} &= f_2 + u_{sq}\,,\\ \frac{\mathrm{d}\phi_{rd}}{\mathrm{d}t} &= f_3 + u_{rd}\,, & \frac{\mathrm{d}\phi_{rq}}{\mathrm{d}t} &= f_4 + u_{rq}\,.\end{aligned} \tag{10}$$

Tacking into account constraint given by (6), one can formulate the Lyapunov function as follows

$$V = \frac{1}{2}\phi_{sd}^2 + \frac{1}{2}\phi_{rq}^2 + \frac{1}{2}\big(\phi_{sq} - \phi_s\big)^2 + \frac{1}{2}\big(\phi_{rd} - \phi_r\big)^2 > 0 \tag{11}$$

where its derivative function becomes

$$\dot V = \phi_{sd}\dot\phi_{sd} + \phi_{rq}\dot\phi_{rq} + \big(\phi_{sq} - \phi_s\big)\big(\dot\phi_{sq} - \dot\phi_s\big) + \big(\phi_{rd} - \phi_r\big)\big(\dot\phi_{rd} - \dot\phi_r\big)\,. \tag{12}$$

Substituting (10) in (12), it results

$$\dot V = \phi_{sd}\big(f_1 + u_{sd}\big) + \phi_{rq}\big(f_4 + u_{rq}\big) + \big(\phi_{sq} - \phi_s\big)\big(f_2 + u_{sq} - \dot\phi_s\big) + \big(\phi_{rd} - \phi_r\big)\big(f_3 + u_{rd} - \dot\phi_r\big)\,. \tag{13}$$

Let us define the following law control as:

$$\begin{aligned}u_{sd} &= -f_1 - K_1\phi_{sd}, & u_{sq} &= -f_2 + \dot\phi_s - K_3\big(\phi_{sq} - \phi_s\big),\\ u_{rq} &= -f_4 - K_2\phi_{rq}, & u_{rd} &= -f_3 + \dot\phi_r - K_4\big(\phi_{rd} - \phi_r\big),\end{aligned} \tag{14}$$

hence (14) replaced in (13) gives:

$$\dot V = -K_1\phi_{sd}^2 - K_2\phi_{rq}^2 - K_3\big(\phi_{sq} - \phi_s\big)^2 - K_4\big(\phi_{rd} - \phi_r\big)^2 < 0\,. \tag{15}$$

The function (15) is negative one. Furthermore, (14) introduced into (10) leads to a stable convergence process if the gains K_i $(i = 1, 2, 3, 4)$ are evidently all positive, otherwise:

$$\begin{aligned}\lim_{t\to+\infty}\phi_{sd} &= 0\,, & \lim_{t\to+\infty}\big(\phi_{rd} - \phi_r^*\big) &= 0\,,\\ \lim_{t\to+\infty}\phi_{rq} &= 0\,, & \lim_{t\to+\infty}\big(\phi_{sq} - \phi_s^*\big) &= 0\,.\end{aligned} \tag{16}$$

In (16), the first and second equations concern the double flux orientation constraints applied for DFIM-model which are define above by (6), while the third and fourth equations define the errors after the feedback fluxes control. This latter offers the possibility to control the main machine magnetizing on the d-axis by ϕ_{rd} and the developed torque on the q-axis by ϕ_{sq}.

C. Torque optimization factor

To optimize the DFIM electromagnetic torque, especially in transient operations, let us calculate the time derivative function of (7) such as we obtain a separable variables fluxes differential equation given as follows

$$\dot\phi_s\phi_r + \dot\phi_r\phi_s = 0\,. \tag{17}$$

In this proposed DFIM control strategy, the limitation of the transient torque goes by the limitation of the stator flux which defines the torque input command component on q-axis. Otherwise, we must assume the following constraint

$$\phi_s \le \phi_{s\max}\,. \tag{18}$$

If (17) and (18), are simultaneously considered, then we can write

$$-\dot\phi_s\phi_r = \dot\phi_r\phi_s \le \dot\phi_r\phi_{s\max} \tag{19}$$

thus,

$$-\frac{\dot\phi_s}{\phi_{s\max}} \le \frac{\dot\phi_r}{\phi_r}\,, \tag{20}$$

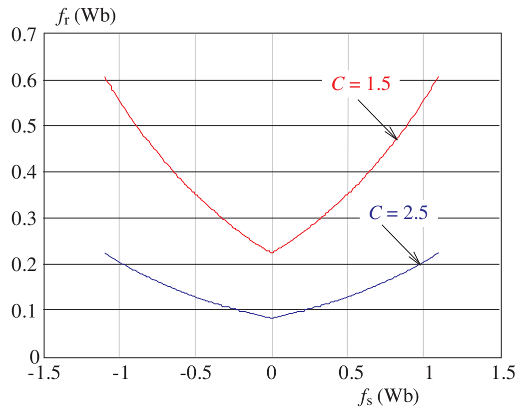

Fig. 3. Fluxes TOF-characteristics.

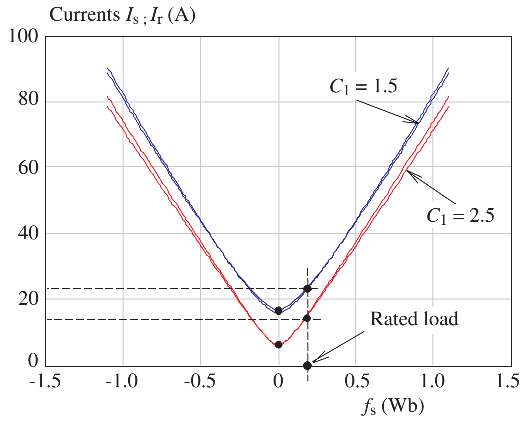

Fig. 4. Currents TOF-characteristics.

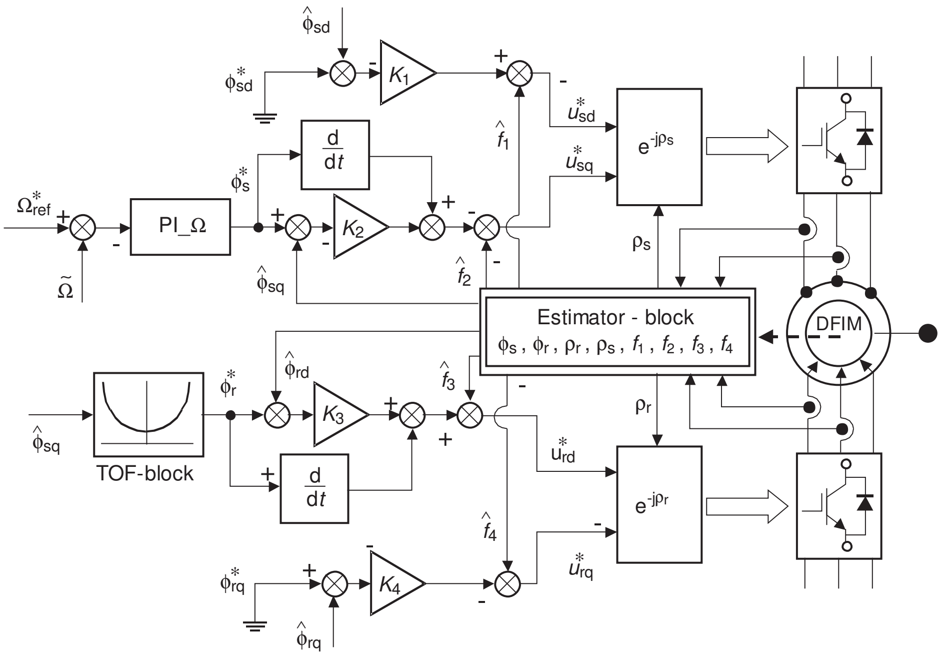

Fig. 5. General block diagram of the suggested DFIM.

the resolution of (20) leads to

$$-\frac{\phi_s}{\phi_{s\,\max}} + C \le \ln \phi_r \tag{21}$$

therefore,

$$\phi_r \ge e^{-\left(\frac{\phi_s}{\phi_{s\,\max}}+C\right)}. \tag{22}$$

Since, the main torque input-command in motoring DFIM operation is related to the stator flux, so it depends of the speed rotor sign, thus we can write

$$\phi_{sq} = \phi_s \operatorname{sgn}\Omega = \begin{cases} +\phi_s & \text{if } \Omega > 0\,, \\ -\phi_s & \text{if } \Omega < 0 \end{cases} \tag{23}$$

with above equation (23), (24) may be rewritten as follows

$$\phi_r = e^{\left(\frac{|\phi_{sq}|}{\phi_{s\,\max}}-C\right)}. \tag{24}$$

The tested laboratory machine parameters and its ratting values are given next in appendix. We remember that in this DFIM control strategy, the stator flux is assumed as input of torque-command. Figure 3 shows an illustration of the relationship (24) and on which we can observe the direct impact of the arbitrary constant C choice. This process is so-called torque-optimization-factor (TOF), where in optimizing the transient's torque; we can avoid the saturation effect and reduce the magnitude of machine currents from which the DFIM efficiency could be clearly enhanced. The curve corresponding to $C = 2.5$, as shown in Fig. 3, characterises an acceptable saturation level than given by $C = 1.5$. In order to avoid over saturation effect into the machine, the maximal stator flux is done at 1.1 Wb and in the same time the rotor flux don't exceed the same value (1.1 Wb), in the all cases. Fig. 4 gives the stator and rotor currents versus input torque command (stator flux) when TOF is used. For $C = 1.5$, the stator and rotor currents represent practically the same curves. Note that $C = 2.5$ gives the reduced magnitude currents

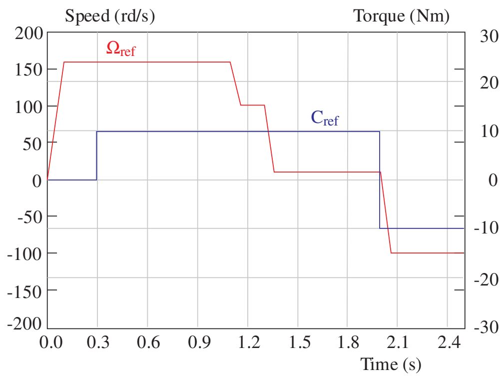

Fig. 6. Speed/torque reference profiles.

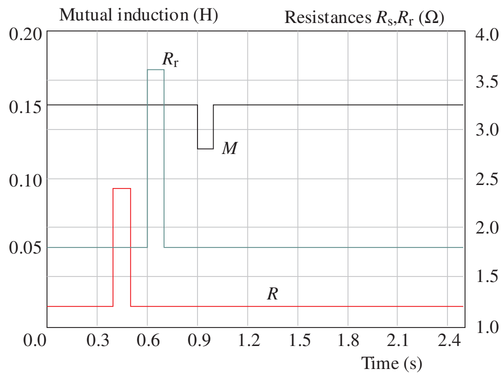

Fig. 7. Parametric profile variations.

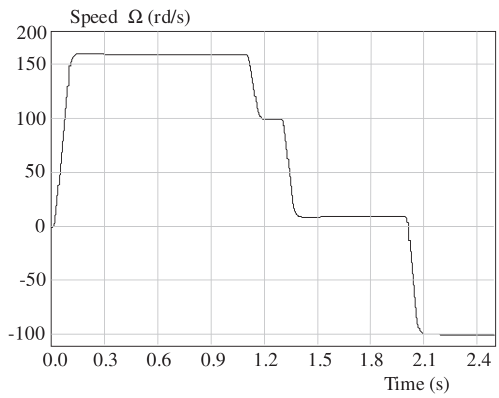

Fig. 8. Speed versus time.

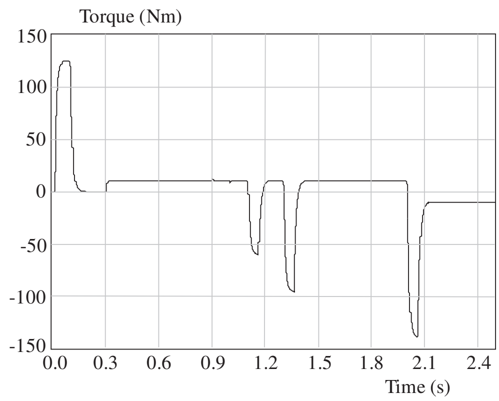

Fig. 9. Torque versus time.

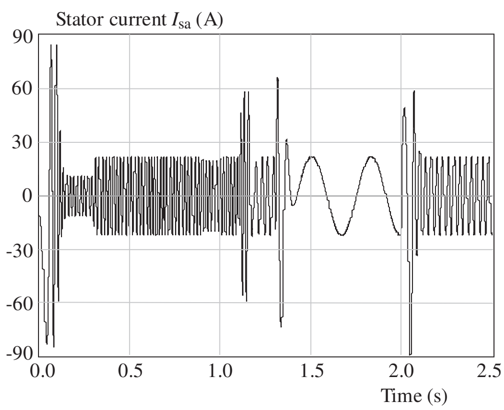

Fig. 10. Stator current versus time.

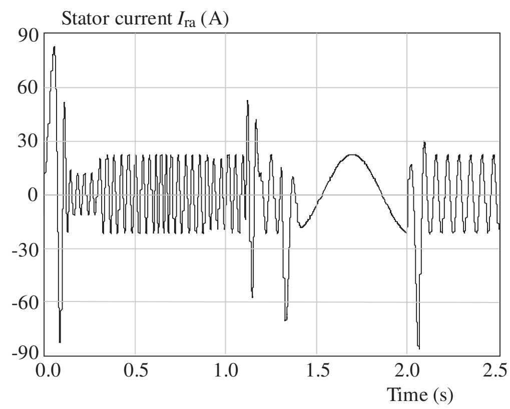

Fig. 11. Rotor current versus time.

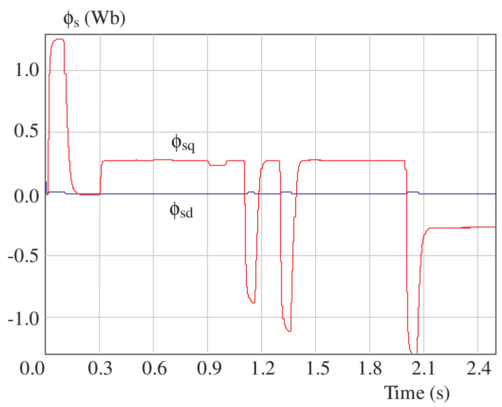

Fig. 12. Stator flux versus time.

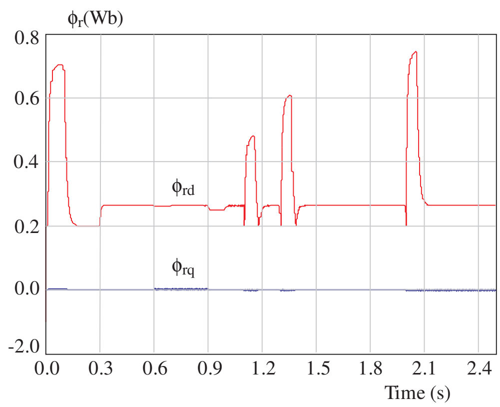

Fig. 13. Rotor flux versus time.

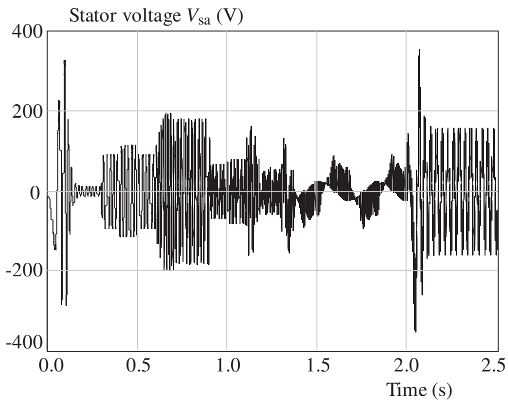

Fig. 14. Stator voltage versus time.

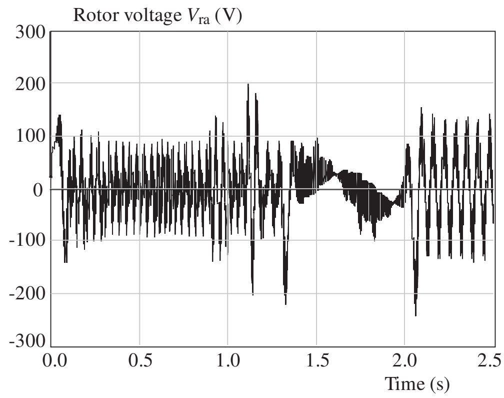

Fig. 15. Rotor voltage versus time.

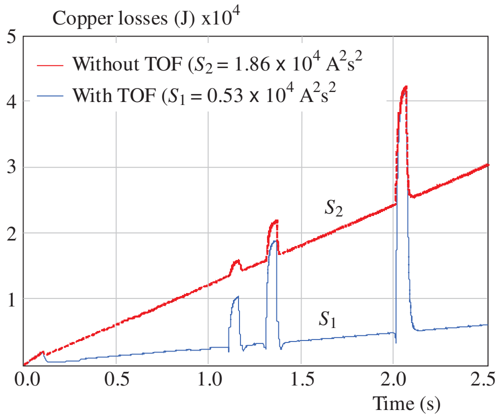

Fig. 16. Total copper losses versus time during test with and.

than $C = 1.5$ for a given load torque corresponding to a given input-command defined by the stator flux. Therefore, a judicious choice of the arbitrary constant C can substantially reduce the currents magnitudes.

Figure 5 illustrates a general block diagram of the suggested DFIM control scheme. As shown in this figure, we can see that only one PI speed controller is used and the fluxes are nonlinear feedback controlled. Also, we can note the placement of TOF-block and the estimator-block which evaluates firstly the modulus and position fluxes, respectively ϕ_s, ϕ_r, ρ_s and ρ_r, from the measured currents using (2) and secondly the feedback functions f_1, f_2, f_3, f_4 given by (9). TOF process allows adapting the main flux magnetizing defined by rotor flux to the applied load torque characterized by the stator flux. Indeed, the energy saving process can be well achieved if the magnetizing flux decreases in the same way that the loads torque. It results equilibrium between the core losses and the copper losses into the machine, so the machine efficiency may be largely improved.

5 SIMULATION

A. Timetable reference profiles

As indicated above, the tested laboratory machine data are given in appendix. In order to validate our approach, the digital simulation has been realized using the general block-diagram given by Fig. 5. We assume to have a timetable of different operating conditions illustrated by the basic profiles defined in Figs. 6 and 7. Hence, the obtained results are organized respectively according to the following specifications. Figure 6 indicates that after 0.3 s of the unloaded machine starting, a load torque corresponding to 10 mN is applied. It is maintained in next simulation even at the reverse speed operation. The proposed DFIM control system has been also tested at very low speed range (at 10 rd/s) as shown in Fig. 6. In Fig. 7, at 0.4 s and 0.6 s the stator and rotor resistances are respectively increased at 100 % of their ratted values, thereafter at 0.9 s the mutual inductance is decreased at 20 % of its ratted value.

B. Test results

Figure 8 shows the speed response versus time according to its desired profile given in Fig. 6. Figure 9 illustrates the electromagnetic torque versus time in good agreement to the applied torque load. So, the observed the torque impulses are naturally developed for the rapid change of speed. Figures 10 and 11 show respectively the stator and the rotor currents versus time occurred during the test. Figures 12 and 13 present the machine fluxes versus time from where we can observe clearly the double flux orientation strategy respecting to the constraints (6). Note the observed flux impulses are due to the above torque impulses. Evidently they are presents in the stator flux which is the input torque command and in rotor flux by the TOF link.

The magnitude of theses flux impulses can be considered as acceptable and they don't solicit strongly the saturation effect. The machine input voltages time evolution is given by Figs. 14 and 15. Figure 16 highlights an interesting contribution of saving energy incarnate by the i^2t of total copper losses time varying when the proposed TOF is used. In this last figure $S_1 = 1.86 \times 10^4\ \mathrm{A^2s^2}$ and $S_2 = 0.53 \times 10^4\ \mathrm{A^2s^2}$ indicate respectively the computed areas limited by both curves defined with and without TOF and, in this situation, the ration energy saving ratio is 3.5 times.

6 CONCLUSION

Access to the stator and rotor windings is one of the advantages of the wound rotor induction machine compared to the conventional squirrel-cage machine. Also, the DFIM offering the several possible combinations for its control. The simulations results of the suggested DFIM system control based in double flux orientation which is achieved by the non linear feed back control demonstrates clearly the suitable obtained performances required according to the references profiles defined above. The speed tracks its desired reference without any effect of both load torque and parameters machine model variation. Therefore the control robustness can be well affirmed. The control flux option, used in this paper, permits to give an optimal torque which is formulated in simpler expression (ideal machine). Energy saving point of view, the copper losses can be substantially reduced using the proposed torque optimization factor (TOF). On other hand, this one allows also to keep the fluxes level at their acceptable magnitudes. The adopted double flux orientation for DFIM used with the nonlinear feedback control and the TOF for energy saving constitute an interesting contribution of this paper in despite that two converters must be employed.

APPENDIX

Parameters	Rated Values	Unity
Output power	4	kW
Stator voltage	220/380	V
Stator frequency	50	Hz
Pole number	2	
Stator resistance	1.2	Ω
Rotor resistance	1.8	Ω
Rotor inductance	0.4612	H
Mutual inductance	0.15	H
Inertia	0.07	$\mathrm{Kg\,m^2}$

References

[1] VICATOS, M. S.—TEGOPOULOS, J. A.: A Doubly-Fed Induction Machine Differential Drive Model for Automobiles, IEEE Transactions on Energy Conversion, **18** No. 2 (2003), 225–230.

[2] HIROFUMI AKAGI—HIKARU SATO: Control and Performance of a Doubly-Fed Induction Machine Intended for a Flywheel Energy Storage System, IEEE Transactions on Power Electronics **17** No. 1 (2002), 109–116.

[3] DEBIPRASAD PANDA—BENEDICT, E. L.—VENKATARAMANAN, G.—LIPO, T. A.: A Novel Control Strategy for the Rotor Side Control of a Doubly-Fed Induction Machine, IEEE (2001), 1695–1702.

[4] LEONHARD, W.: Control Electrical Drives, Springier Verlag, Berlin, Heidelberg, 1997.

[5] WANG, S.—DING, Y.: Stability Analysis of Field Oriented Doubly Fed Induction Machine Drive Based on Computed Simulation, Electrical Machines and Power Systems (Taylor & Francis), 1993.

[6] MOREL, L. *et al*: Double-Fed Induction Machine: Converter Optimisation and Field Oriented Control without Position Sensor, IEE Proc. Electr. Power Appl. **145** No. 4 (1998).

[7] HOPFENSPERGER, B. *et al*: Stator Flux Oriented Control of a Cascaded Doubly Fed Induction Machine, IEE Proc. Electr. Power Appl. **146.** No. 6 (1999).

[8] HOPFENSPERGER, B. *et al*: Stator Flux Oriented Control of a Cascaded Doubly Fed Induction Machine with and without Position Encoder, IEE Proc. Electr. Power Appl. **147** No. 4 (1999), 241–250.

[9] METWALLY, H. M. B. *et al*: Optimum Performance Characteristics of Doubly Fed Induction Motors Using Field Oriented Control, Energy Conversion and Management **43** (2002), 3–13.

[10] DATTA, R.—RANGANATHAN, V. T.: A Simple Position Sensorless Algorithm for Rotor Side Field Oriented Control of Wound Rotor Induction Machine, IEEE Trans. Ind. Electron. **48** (2001), 786–793.

[11] DJUROVIC, M. *et al*: Double Fed Induction Generator with Two Pair of Poles, Conferences of Electrical Machines and Drives (IEMDC), 11-13 September 1995, Conference Publication, No. 412 IEE 1995.

[12] KELBER, C.—SCHUMACHER, W.: Adjustable Speed Constant Frequency Energy Generation with Doubly Fed Induction Machines, European Conference of Variable Speed in Small Hydro (VSSHy), in Grenoble, 2000.

[13] KELBER, C.—SCHUMACHER, W.: Control of Doubly fed induction Machine as an Adjustable Motor/Generator, European Conference of Variable Speed in Small Hydro (VSSHy), in Grenoble, 2000.

[14] LONGYA XU—WEI CHENG: Torque and Reactive Power Control of a Doubly Fed Induction Machine by Position Sensorless Scheme, IEEE Transactions on Industry Applications **31** No. 3 (1995), 636–642.

[15] PERESADA, S.—TILLI, A.—TONIELLI, A.: Indirect Stator Flux-Oriented Output Feedback Control of a Doubly Fed Induction Machine, IEEE Trans. On Control Systems Technology **11** (2003), 875–888.

Received 1 October 2004

Saïd Drid, born in Batna, Algeria, in 1969, received the BSc degree in electrical engineering from the University of Batna, Algeria, in 1994, and the MSc degree in electrical and computer engineering from the Electrical Engineering Institute of Batna University, Algeria, in 2000. Since graduation, he has been with the University of Batna, Algeria sa teaching assistant at the Electrical Engineering Institute.

Mohamed Tadjine, born in Algiers, Algeria, in 1966, received the BEng degree in automatic control from the National Polytechnic Institute of Algiers, Algeria, in 1990, and the PhD degree in control systems from the Institute National Polytechnic of Grenoble, France, in 1994. He is currently with the Department of Automatic Control, National Polytechnic Institute of Algiers, Algeria.

Mohamed-Said Nait-Said, born in Batna, Algeria, in 1958, received the BSc degree in electrical engineering from the National Polytechnic Institute of Algiers, Algeria, in 1983, and the MSc degree in electrical and computer engineering from the Electrical Engineering Institute of Constantine University, Algeria, in 1992. He received the PhD degree in electrical and computer engineering from the University of Batna in 1999 and currently is Full Professor at the Electrical Engineering Institute at the University of Batna.